NASA TECHNICAL NOTE

CREEP DEGRADATION IN OXIDE-DISPERSION-STRENGTHENED ALLOYS

J. Daniel Whittenberger

Lewis Research Center
Cleveland, Ohio 44135

NATIONAL AERONAUTICS AND SPACE ADMINISTRATION • WASHINGTON, D. C. • MARCH 1977

1. Report No. NASA TN D-8421	2. Government Accession No.	3. Recipient's Catalog No.
4. Title and Subtitle CREEP DEGRADATION IN OXIDE-DISPERSION-STRENGTHENED ALLOYS		5. Report Date March 1977 6. Performing Organization Code
7. Author(s) J. Daniel Whittenberger		8. Performing Organization Report No. E-8849
9. Performing Organization Name and Address Lewis Research Center National Aeronautics and Space Administration Cleveland, Ohio 44135		10. Work Unit No. 505-01 11. Contract or Grant No.
12. Sponsoring Agency Name and Address National Aeronautics and Space Administration Washington, D.C. 20546		13. Type of Report and Period Covered Technical Note 14. Sponsoring Agency Code
15. Supplementary Notes		

16. Abstract

A study was undertaken to determine if oxide-dispersion-strengthened (ODS) Ni-base alloys in wrought bar form are subject to creep degradation effects similar to those found in thin-gage sheet. The bar products evaluated included ODS-Ni, ODS-NiCr, and three types of advanced ODS-NiCrAl alloys. Tensile test specimens were exposed to creep at various stress levels at 1365 K and then tensile tested at room temperature. Low residual tensile properties, change in fracture mode, the appearance of dispersoid-free bands, grain boundary cavitation, and internal oxidation in the microstructure were interpreted as creep degradation effects. This work showed that many ODS alloys are subject to creep damage. Degradation of tensile properties occurred after very small amounts ($\lesssim$0.2 percent) of creep strain, ductility being the most sensitive property. The amount of degradation was dependent on the creep strain and was essentially independent of the alloy system. All the ODS alloys which were creep damaged possessed a large grain size (>100 μm). Creep damage appears to have been due to diffusional creep which produced dispersoid-free bands around boundaries acting as vacancy sources. Low angle and possibly twin boundaries acted as vacancy sources. The residual tensile properties of two alloys were not affected by prior creep parallel to the extrusion axis. One of these alloys, DS-NiCr(S), was a single crystal. The other alloy, TD-Ni, possessed a small, elongated grain structure, which minimized the thickness of the dispersoid-free bands produced by diffusional creep.

17. Key Words (Suggested by Author(s)) Creep; Creep degradation; Dispersion strengthened alloys; Oxide dispersion strengthened; ODS	18. Distribution Statement Unclassified - unlimited STAR Category 26		
19. Security Classif. (of this report) Unclassified	20. Security Classif. (of this page) Unclassified	21. No. of Pages 36	22. Price* A03

* For sale by the National Technical Information Service, Springfield, Virginia 22161

CONTENTS

CREEP DEGRADATION IN OXIDE-DISPERSION-STRENGTHENED ALLOYS

by J. Daniel Whittenberger

Lewis Research Center

SUMMARY

A study was undertaken to determine if oxide-dispersion-strengthened (ODS) Ni-base alloys in wrought bar form are subject to creep degradation effects similar to those found in thin-gage sheet. The bar products evaluated included ODS-Ni, ODS-NiCr, and three types of advanced ODS-NiCrAl alloys. Tensile test specimens were exposed to creep at various stress levels at 1365 K and then tensile tested at room temperature. Low residual tensile properties, change in fracture mode, the appearance of dispersoid-free bands, grain boundary cavitation, and internal oxidation in the microstructure were interpreted as creep degradation effects. This work showed that many ODS alloys are subject to creep damage. Degradation of tensile properties occurred after very small amounts ($\lesssim$0.2 percent) of creep strain, ductility being the most sensitive property. The amount of degradation was dependent on the creep strain and was essentially independent of the alloy system. All the ODS alloys which were creep damaged possessed a large grain size (>100 μm). Creep damage appears to have been due to diffusional creep, which produced dispersoid-free bands around boundaries acting as vacancy sources. Low angle and possibly twin boundaries acted as vacancy sources. The residual tensile properties of two alloys were not affected by prior creep parallel to the extrusion axis. One of these alloys, DS-NiCr(S), was a single crystal. The other alloy, TD-Ni, possessed a small, elongated grain structure, which minimized the thickness of the dispersoid-free bands produced by diffusional creep.

INTRODUCTION

Recent work (ref. 1) has shown that thin-gage sheet of the oxide-dispersion-strengthened (ODS) alloy TD-NiCr (Ni-20Cr-2ThO_2) is subject to creep degradation. Small amounts of creep (less than 1 percent) at elevated temperatures (1144 to 1477 K) produced intergranular damage which severely reduced room temperature tensile properties, tensile ductility being particularly affected. It has been proposed (ref. 2) that

this creep damage is the result of diffusional creep, which produces dispersoid-free bands on grain boundaries acting as vacancy sources. Such dispersoid-free bands are weak compared with the original ODS alloy. In addition, the bands can act as sites for cavitation and intergranular oxidation, which further weaken the alloy. These observations suggest that most ODS alloys should be susceptible to this type of creep damage.

The purpose of this study was to determine if ODS Ni-base alloys in wrought bar form are subject to creep degradation effects similar to those found in thin-gage sheet. Such behavior is of interest as ODS alloys are being considered for use as vanes in advanced gas turbine engines. The bar products evaluated included ODS-Ni, ODS-NiCr, and three types of advanced ODS-NiCrAl alloys. Tensile test specimens were exposed to creep at various stress levels at 1365 K and then tensile tested at room temperature. Low residual tensile properties, change in fracture mode, the appearance of dispersoid-free bands, grain boundary cavitation, and internal oxidation in the microstructure were interpreted as creep degradation effects.

EXPERIMENTAL PROCEDURE

The five ODS alloys evaluated and their chemical compositions are shown in table I. Two alloys were obtained from Fansteel, Inc.: TD-Ni in the form of heat-treated (stress-relieved) bar with a 1.27-centimeter diameter and TD-NiCrAl as an upset steel canned billet with a 20-centimeter diameter. DS-NiCr was provided by the Cabot Corporation as unrecrystallized sheet bar with a 1.9- by 6.4-centimeter cross section. Inconel MA-754 was purchased from Huntington Alloys, Inc., in the form of heat-treated sheet bar with a 2.8- by 9.3-centimeter cross section. The experimental alloy DST-NiCrAl was obtained from Sherritt-Gordon Mines Ltd. in the form of pressed and sintered billets 7.6 centimeters in diameter. DS-NiCr was divided into two lots, and each lot was given a different recrystallization heat treatment. The alloys in billet form were subjected to various thermal mechanical processing and heat treatment schedules in order to obtain an elongated microstructure with a uniform, large grain size. The known processing and heat treatment schedules for the ODS alloys are shown in table II. DS-NiCr, TD-NiCrAl, and DST-NiCrAl were tested after being subjected to the processing and heat treatment schedules shown in table II. TD-Ni and Inconel MA-754 were tested in the as-received condition. In this work, the condition of the alloys prior to testing is termed the as-received condition.

The average grain size parameters as determined by lineal analysis and the crystallographic texture of the as-received alloys are given in table III. Of the alloys evaluated in this study, DS-NiCr possessed the most unusual structure, as the heat-treated bars were single crystals. The two different heat treatments did, however, produce different macrostructures, as shown in the macroetched sections in figure 1. Because of their

unique microstructures, grain aspect ratios could not be determined for the DS-NiCr bars. Of the other alloys tested, only TD-Ni possessed a high grain aspect ratio. Neither average particle size nor interparticle spacing was determined for any of these alloys.

Round bar tensile specimens with a gage section nominally 2.8 centimeters long by 0.51 centimeter in diameter were centerless ground from the heat-treated alloys. In general, tapered grip specimens were used; however, threaded grip end specimens were used for DS-NiCr(S) tested in the long transverse direction and for Inconel MA-754 in order to conserve material. All alloys were tested parallel to the extrusion axis; in addition, DS-NiCr(S) and Inconel MA-754 were tested in the long transverse direction.

All creep testing was conducted at 1365 K in air on constant-load test machines. Creep tests were designed to produce from 0.1 to 1.0 percent total creep (transient plus steady-state plus tertiary, if any) in nominally 100 hours. Elongation as a function of time was measured optically from scribed platinum strips which had been spot welded to the shoulders of the test specimens. At the completion of a creep test, the furnace was turned off, and the stress was reduced at least 50 percent. After cooling, the creep-tested specimens were tensile tested at room temperature. Also, with a few exceptions, duplicate as-received alloy specimens were tensile tested at room temperature. Tensile testing was conducted on an oil-operated hydraulic test machine at a cross-head speed of about 0.001 centimeter per second with strain through the 0.2 percent yield strength measured by a clip-on extensometer.

All residual tensile properties were calculated on the basis of the original (as-received) cross-sectional area. The 0.2 percent yield strengths measured on creep-tested specimens are somewhat suspect since the gage sections of all these specimens were oxidized. Following tensile testing, selected residual property and as-received specimens were subjected to additional examination including metallography and scanning electron microscope (SEM) fractography. While this report emphasizes the effect of prior creep on room temperature residual tensile properties, a limited examination of the effect of prior creep on elevated temperature tensile properties was also made (appendix A).

RESULTS

This report is concerned with the room temperature residual tensile properties after creep testing. Only those mechanical property data necessary to discuss residual properties are presented. A general discussion of the tensile properties and creep characteristics of the alloys at 1365 K is presented in reference 3.

The creep history and residual tensile properties for all the alloys are given in table IV. In general, the following were interpreted as effects of creep degradation:

(1) Low tensile ductility compared with as-received value

(2) Low ultimate tensile strength compared with as-received value

(3) Changes in macroscopic fracture appearance, usually from intragranular (as-received) to intergranular (creep-damaged)

(4) Differences in SEM fractography between as-received and residual fracture surfaces

(5) Intergranular cracking, significant numbers of creep cavities, internal oxidation, and dispersoid-free bands in residual property specimens

Applying the first three indicators to the residual property data in table IV reveals that six of the eight alloy-direction combinations were subject to creep degradation at very low strains (of the order of 0.2 percent creep). They are DS-NiCr(S) and Inconel MA-754 tested in the long transverse direction and DS-NiCr(F), Inconel MA-754, TD-NiCrAl, and DST-NiCrAl tested parallel to the extrusion axis. DS-NiCr(S) tested parallel to the extrusion axis was apparently free of creep degradation effects up to 1.6 percent creep strain. TD-Ni tested parallel to the extrusion axis was also not subject to degradation, at least up to approximately 0.4 percent creep; however, the decrease in ultimate tensile strength of the TD-Ni specimen subjected to 0.49 percent creep indicates that higher strains might result in degradation.

SEM fractography techniques and metallography of the eight alloy-direction combinations confirmed that only DS-NiCr(S) and TD-Ni tested parallel to the extrusion axis were not affected by prior creep. Figure 2 illustrates typical examples of as-received and creep-damaged fracture surfaces. The lacy-network surface which is formed by the outline of very large fracture dimples shown in figure 2(b) was observed on the tensile fracture surface of all the alloys which were creep damaged. This type of surface is identical to that found on creep-damaged TD-NiCr (ref. 1). All fracture surfaces of creep-damaged specimens contain areas of the as-received type surface (similar to fig. 2(a)) and the lacy-network surface (fig. 2(b)). In addition, many residual specimens subjected to creep strains greater than about 0.4 percent contained oxidized regions. Metallography of selected residual property specimens revealed that tensile failure was basically intergranular in creep-damaged specimens, while undamaged (as-received) specimens underwent intragranular tensile failure. Also, many creep-tested specimens contained significant intergranular damage such as cracking, cavities, and dispersoid-free bands; the extent of this intergranular damage increased with increasing creep strain. A typical example of intergranular damage is shown in figure 3. Additional documentation of creep degradation is presented in appendix B.

DISCUSSION

From the residual property data presented in table IV, it is apparent that most ODS alloys tested in this study sustained creep degradation during tensile creep at 1365 K. As can be seen in figure 4, which presents plots of normalized room temperature tensile properties (residual value/as-received value) as a function of creep strain, the extent of creep damage is dependent on the strain and essentially independent of the composition, grain size, and grain aspect ratio of the alloy system. The data in this composite figure indicate that significant reduction (>10 percent) in the room temperature ultimate tensile strength requires at least 0.4 percent creep strain; on the other hand, large reductions in room temperature ductility can occur at 0.2 percent creep strain or less. Therefore, tensile ductility is a much more sensitive indicator of creep damage than ultimate tensile strength.

It has been proposed (ref. 1) that creep damage in polycrystalline Ni-base alloys is the result of diffusional creep. In order for this to be true, diffusional creep mechanisms must make a significant contribution to creep in these alloys. Because of the absolute theoretical models of diffusional creep, diffusional creep rates can be calculated for ODS-Ni, and these rates can be compared with actual creep rates for typical ODS alloys. From Raj and Ashby's work (refs. 4 and 5), the combined creep rate $\dot{\epsilon}$ due to the diffusional creep mechanisms is

$$\dot{\epsilon} = 14 \frac{\Omega D_V}{kT} \frac{\sigma}{d^2} + 44 \frac{\delta \Omega D_B}{kT} \frac{\sigma}{d^3} \tag{1}$$

where Ω is the atomic volume, k is Boltzmann's constant, T is the absolute temperature, D_V is the volume diffusion coefficient, D_B is the grain boundary diffusion coefficient, δ is the grain boundary width, σ is the applied stress, and d is the equiaxed grain size. From this equation the stress, temperature, and grain size necessary to produce 1 percent creep in 100 hours can be calculated for ODS-Ni where (from ref. 6)

$$D_V = 6.6 \times 10^{-5} \exp\left(-\frac{255\,000}{RT}\right) \tag{2}$$

$$D_B = 1.1 \times 10^{-5} \exp\left(-\frac{124\,100}{RT}\right) \tag{3}$$

(where D_V and D_B are in m^2/sec and $R = 8.314$ J/(kmole)(K)) and

$$\Omega = 10^{-29}\ m^3$$

$$\delta = 10^{-9}\ m$$

In figure 5, the theoretical stress and temperature conditions to produce 1 percent creep in 100 hours in ODS-Ni with a 250-micrometer grain size are compared with nominal 100-hour stress-rupture strengths for advanced Ni-base ODS alloys (ref. 7). Since these alloys generally exhibit 1 percent strain prior to rupture, the 100-hour rupture stress is a reasonable approximation of the stress to produce 1 percent creep in 100 hours. In addition, a 250-micrometer grain size is typical of many advanced ODS alloys: for example, Inconel MA-754 and TD-NiCrAl which were tested in this study. Figure 5 reveals that the actual strength of the advanced ODS alloys is greater than the theoretical diffusional creep strength for temperatures of 1255 K or more. From this figure it can be seen that diffusional creep is possible and that it can more than account for the creep deformation that is experimentally observed. The difference between actual strength and theoretical strength could be due, in part, to a threshold stress for creep (refs. 1 and 2). Although the theoretical curve in figure 5 is for an ODS-Ni alloy, solid solution Ni-base alloys would exhibit almost identical curves of strength as a function of temperature since diffusion in nickel solid solutions is not greatly influenced by normal alloying additions.

As diffusional creep seems to be a viable creep mechanism in polycrystalline ODS-Ni alloys, one must consider its effect on the microstructure, in particular, the growth of dispersoid-free bands around grain boundaries acting as vacancy sources since these appear to be directly responsible for creep degradation. Figure 6 illustrates various theoretical stress, temperature, and time conditions necessary to produce a 2-micrometer-thick dispersoid-free band for two grain sizes. These curves indicate that moderate stresses can rather quickly form significant dispersoid-free bands in either 100- or 500-micrometer-grain-size material. For most ODS-Ni alloys a 2-micrometer-thick dispersoid-free band is a region which is at least an order of magnitude wider than the average interparticle spacing; therefore, these bands will be considerably weaker than the dispersion-strengthened portion of the microstructure. In general, one would expect the material in wide dispersoid-free bands to behave as a normal solid solution and to be subject to normal creep processes such as dislocation climb/glide and cavity formation. Finally, it should be noted that the width w of dispersoid-free bands is dependent on the diffusional creep strain ϵ and equiaxed grain size d, where

$$\epsilon = \frac{w}{d} \tag{4}$$

Thus, small strains and small grain size would result in narrow dispersoid-free bands, while small strains and large grain size would result in wide bands: for example, 0.4 percent creep strain in 25- and 250-micrometer-grain-size alloys would produce 0.1- and 1-micrometer-thick dispersoid-free bands, respectively.

The diffusional creep model (ref. 1) of creep degradation agrees well with the results of this study. With regard to the six combinations of alloy, heat treatment, and direction which exhibited creep degradation (fig. 4), metallography revealed the presence of a large grain size and transverse boundaries in the test sections of the alloys in these combinations. Apparently at least some of the transverse boundaries acted as vacancy sources during tensile creep. In general, the boundaries in the alloys in these combinations were not normal high-angle grain boundaries as all the alloys possessed texture (table III). Thus, it appears that tensile creep conditions can force low-angle grain boundaries and possibly even twin boundaries such as occurred in DS-NiCr(F) to act as vacancy sources.

Creep degradation was not observed in either TD-Ni or DS-NiCr(S) when they were tested parallel to the extrusion axis. This is also interpretable by assuming that diffusional creep is responsible for creep degradation. DS-NiCr(S) tested parallel to the extrusion axis does not contain transverse boundaries as it is essentially a perfect single crystal in this direction. On the other hand, TD-Ni contains many transverse grain boundaries; however, because of the small grain size ($\sim$3 μm) only very narrow dispersoid-free bands would be formed during creep. Narrow bands should not affect the residual tensile properties.

During the course of this study, it was observed that all of the alloy-direction combinations possessed threshold stresses for creep (ref. 3). Prior creep exposure at stress levels equal to or below the threshold stress did not cause creep degradation. Thus, maintaining applied stresses below the threshold stress for creep offers the best potential for avoiding creep degradation. Microstructural control, as suggested by the test results for DS-NiCr(S) and TD-Ni, is probably not practical. Single-crystal material must be perfect (without subgrain boundaries) in order to be completely free of diffusional creep. TD-Ni is the only known practical example of a strong, small grain size ODS-Ni alloy; all other ODS-Ni alloys with a small grain size are extremely weak.

These results seem to indicate that use of ODS alloys should be limited to low stress applications where creep is unlikely to occur. For example, ODS alloys have shown excellent potential for aircraft turbine engine vanes (ref. 8). In this application, resistance to oxidation and sulfidization, thermal fatigue, and overtemperature capability are of primary importance, while only moderate strength is required. Should creep degradation occur in ODS alloy vanes, thermal fatigue behavior would probably be affected. However, problems of this type have not been observed in actual engine tests of ODS alloy vanes, probably because of the relatively low stress experienced by vanes.

Finally, figure 4 demonstrates a straightforward, simple relation between creep degradation and prior creep; a similar relation between creep strain and applied creep stress is not possible. Reexamination of the creep history data in table IV demonstrates that considerable differences in the creep strength properties exist. For example, the stresses required to produce approximately 0.3 percent creep in 150 hours at 1365 K range from about 50 MPa for TD-NiCrAl and DST-NiCrAl to about 70 MPa for DS-NiCr(S) and Inconel MA-754 for alloys tested parallel to the extrusion axis, while Inconel MA-754 tested in the long transverse direction only requires about a 20-MPa stress. It is probable that some of the observed differences in strength are due to grain size and grain aspect ratio effects; in addition, part of the strength differences could be due to differences in the threshold stress (refs. 3, 9, and 10) for creep for the various alloy systems and test directions.

CONCLUSIONS

Based on a study of creep degradation in ODS-Ni alloys, it is concluded that ODS alloys possessing a large grain size separated by high angle, low angle, and/or twin boundaries must be limited to stress and temperature conditions where creep essentially will not occur (strains $\lesssim$0.2 percent) in order to avoid significant creep damage. Degradation appears to be due to diffusional creep, which produces dispersoid-free bands around grain boundaries acting as vacancy sources.

Lewis Research Center,
National Aeronautics and Space Administration,
Cleveland, Ohio, December 3, 1976,
505-01.

APPENDIX A

EFFECT OF CREEP IN ODS ALLOYS ON 1365 K RESIDUAL TENSILE PROPERTIES

Following creep testing at 1365 K, selected specimens of TD-NiCrAl and DST-NiCrAl were tensile tested at 1365 K to assess the effects of prior creep deformation on elevated temperature mechanical properties. Creep-tested specimens and duplicate as-received specimens were tensile tested in air at 1365 K at a constant cross-head speed of 0.0021 centimeter per second. All tensile properties were calculated on the basis of as-received cross section, and the 0.2 percent offset yield strength was estimated from the chart for load and cross-head speed. Following tensile testing, several specimens were metallographically examined. SEM fractography of the fracture surfaces was attempted; however, oxidation obliterated practically all details.

The creep histories and 1365 K residual tensile properties of the ODS alloys tested are shown in table V. For TD-NiCrAl prior creep had apparently little effect on the tensile strength properties; however, the macroscopic fracture mode and tensile ductility were influenced by very small (~0.1 percent) amounts of creep. Metallographic evidence of creep damage can be seen in figure 7, where the tensile failure has been changed from intragranular fracture in the as-received specimens to partial intergranular fracture in the creep-damaged specimen. Part of this degradation could be due to intergranular carbides (TD-NiCrAl contained ~0.05 wt. % C); however, carbides can not account for all the degradation since specimen TL-8 had tensile properties almost equal to the as-received values.

Prior creep in DST-NiCrAl also had little effect on 1365 K tensile strength properties, but some reduction in tensile elongation could be seen. Metallographic examination of tested specimens revealed that both the as-received and creep-tested specimens suffered intergranular failure; in addition, definite signs of intergranular damage produced by creep were seen in the creep-tested specimens; a typical example is shown in figure 8. Here the light shading around the cracked boundary is due to alloy depletion, and the large particles near the cracked boundary are oxides. This type of damage is typical of ODS alloys subjected to relatively high creep strains and has been seen in specimens following room temperature residual tensile testing. Apparently, creep damage does not have as great an influence on 1365 K residual tensile properties of DST-NiCrAl as it does on room temperature residual properties since 1365 K tensile fracture is itself intergranular.

From this study of the effects of creep degradation on the 1365 K residual tensile properties of ODS alloys, it appears that (1) prior creep, at least up to about 0.5 percent, has little effect on the residual tensile strength properties; (2) small creep strains

can significantly reduce the tensile ductility if the as-received fracture is intergranular; and (3) tensile ductility is somewhat reduced by prior creep if the as-received fracture is intergranular.

APPENDIX B

ADDITIONAL EVIDENCE OF CREEP DEGRADATION IN ODS ALLOYS

Specific comments on and supporting evidence for the presence or absence of creep degradation for the eight combinations of ODS alloy, heat treatment, and direction tested in this study are given in this appendix.

TD-Ni

As shown in table IV, the residual tensile tests of uncoated TD-Ni revealed no evidence of creep damage. The ultimate tensile strength (UTS) and ductility of the creep-tested specimens (creep strain up to about 0.4 percent) were equivalent to those of the as-received alloy. Good retention of the UTS is somewhat surprising as TD-Ni is not an oxidation resistant alloy at 1365 K. The only possible example of creep degradation was specimen N-50, which experienced 0.49 percent creep; however, the residual ductility was high, while the UTS was 20 percent lower than the as-received value. Neither SEM fractrography nor metallography revealed differences between creep-tested and as-received specimens. Typical SEM fractographs are shown in figure 9 for as-received and creep-exposed specimens.

Finally, the data in table IV on coated TD-Ni reveal that the coating did not affect either the creep or residual tensile properties, which were both equivalent to those of uncoated TD-Ni.

Inconel MA-754

Tested parallel to extrusion axis. - The residual property data in table IV show that Inconel MA-754 tested parallel to the extrusion axis was not degraded up to creep strains of about 0.2 percent. At higher creep strains, the low residual ductility indicates creep degradation. SEM fractography of selected specimens revealed that creep damage occurred at creep strains greater than 0.2 percent. The fractographs in figure 2 are typical of room temperature tensile fracture in as-received and creep-damaged specimens. In addition, residual property specimens subjected to creep strains greater than about 0.4 percent contained areas of oxide on the fracture surface. Metallography of specimens with creep strains greater than 0.2 percent revealed grain boundary cavities and occasional Y_2O_3-free zones.

Tested in long transverse direction. - Inconel MA-754 tested in the long transverse direction possessed the least resistance to creep degradation of any of the combinations of ODS alloy, heat treatment, and direction examined. The data in table IV show that even creep strains of the order of 0.1 percent produced some degradation. Typical SEM fractographs of the room temperature tensile fractures of as-received and creep-damaged test specimens are presented in figure 10. The linear nature of the lacy network array of large fracture dimples shown in figure 10(b) is unique to Inconel MA-754 tested in the long transverse direction; lacy network fracture surfaces found in the other alloys were much more random in appearance (see fig. 2(b)).

DS-NiCr(S)

Tested parallel to extrusion axis. - The residual property data in table IV for DS-NiCr(S) tested parallel to the extrusion axis reveal that this alloy-orientation combination was not susceptible to creep degradation effects, at least up to ~1.6 percent strain. This behavior was expected as specimens taken parallel to the extrusion axis are single crystals. Metallography of tested specimens revealed an occasional subgrain boundary parallel to the gage length. Apparently, subgrain boundaries of this orientation had no effect on residual properties. SEM fractography of as-received and residual property specimens revealed identical fracture surfaces. A typical SEM fractograph is presented in figure 11.

Tested in long transverse direction. - Testing of DS-NiCr(S) in the long transverse direction was conducted in order to evaluate the consequences of transverse subgrain boundaries. The creep histories and residual property results for this material-direction combination are shown in table IV. These data indicate that creep strains up to 0.15 percent will not affect residual properties; however, 0.32 percent creep strain produced a definite decrease in tensile ductility and a change in the outward fracture appearance. SEM fractography of the specimen which experienced 0.32 percent creep revealed that creep damage had taken place. Typical SEM fractographs of as-received and creep-damaged specimens are shown in figure 12.

DS-NiCr(F)

DS-NiCr(F) given an isothermal heat treatment at 1640 K produced an overall structure that was quite similar to that of DS-NiCr(S) except that DS-NiCr(F) had a smaller subgrain size and contained many grains in a twin orientation. The residual property data in table IV indicate that creep degradation is possible at relatively low (0.19 percent) creep strain. An example of a creep-damaged region in specimen F-6 is shown in

figure 13. Fractography of room temperature tensile failure in as-received DS-NiCr(F) was identical to that of DS-NiCr(S).

TD-NiCrAl

The data in table IV indicate that TD-NiCrAl tested parallel to the extrusion axis can be creep damaged. Typical SEM fractographs of room temperature residual property specimens are shown in figure 14. The fracture surface shown in figure 14(a) is typical of an as-received fracture surface except for the dark, flat particles. These particles have been tentatively identified as chromium carbides which precipitate during exposure to elevated temperature. Figure 14(b) illustrates a network of large fracture dimples which is typical of creep damage in ODS alloys.

DST-NiCrAl

Creep histories and room temperature residual tensile properties are given in table IV for DST-NiCrAl tested parallel to the extrusion axis. The room temperature residual properties indicate that creep degradation took place at creep strains as low as 0.3 percent and possibly lower. Metallographic examination revealed that the specimens which experienced 0.38 and 0.68 percent creep strain possessed partially intergranular tensile fracture while the as-received tensile fracture was totally intragranular. SEM fractography provided additional evidence of creep damage. Typical SEM fractographs of as-received and creep-damaged room temperature tensile specimens are shown in figure 15.

Figure 16 illustrates the type of creep damage that occurs at creep strains of the order of 0.5 percent. The dark shaded region near the fracture surface is composed of large chromium and aluminum oxide particles, and the light shading around these oxides is due to alloy depletion.

REFERENCES

1. Whittenberger, John D.: Observations on the Relationship of Structure to the Mechanical Properties of Thin TD-NiCr Sheet. Metall. Trans., vol. 7A, no. 5, May 1976, pp. 611-619.

2. Whittenberger, John D.: Diffusional Creep and Creep-Degradation in Dispersion-Strengthened Ni-Cr Base Alloys. Metall. Trans., vol. 4, no. 6, June 1973, pp. 1475-1483.

3. Whittenberger, J. Daniel: Creep and Tensile Properties of Several Oxide-Dispersion-Strengthened Nickel-Base Alloys at 1365 K. NASA TN D-8422, 1977.

4. Raj, R.; and Ashby, M. F.: On Grain Boundary Sliding and Diffusional Creep. Metall. Trans., vol. 2, no. 4, April 1971, pp. 1113-1127.

5. Ashby, M. F.: A First Report on Deformation-Mechanism Maps. Acta. Metall., vol. 20, no. 7, July 1972, pp. 887-897.

6. Paul, A. R.; and Agarwall, R. P.: Lattice and Grain Boundary Diffusion of Cerium and Neodymium in Nickel. Metall. Trans., vol. 2, no. 9, Sept. 1971, pp. 2691-2695.

7. Blankenship, C. P.: Trends in High Temperature Material Technology for Advanced Aircraft Turbine Engines. SAE Paper 751050, Nov. 1975.

8. Bailey, P. G.: Oxide Dispersion Strengthened Alloys for Aircraft Turbine Engine Vanes. Sixth National Technical Conference for Materials on the Move. Soc. for the Advancement of Material and Process Engr., 1974, pp. 208-217.

9. Lund, R. W.; and Nix, W. D.: High Temperature Creep of Ni-20Cr-2ThO_2 Single Crystals. Acta Metall., vol. 24, no. 5, May 1976, pp. 469-481.

10. Lin, J.; and Sherby, O. D.: Mechanical Behavior of Dispersion Hardened Materials at Elevated Temperatures. SAR-2, Stanford Univ., 1975.

TABLE I. - NOMINAL ALLOY CHEMISTRY

Alloy	Cr	Al	C	ThO_2	Y_2O_3	Ni
	Concentration, wt. %					
TD-Ni (heat 3062)	----	---	0.027	2	---	Bal.
DS-NiCr	20.3	---	.009	2	---	↓
Inconel MA-754[a] (heat 0T0055B)	20	0.6	.07	-	0.6	↓
TD-NiCrAl (heat 3939)	16	4.2	.05	2	---	↓
DST-NiCrAl	16	5	.013	2	---	↓

[a]Also contains 1.5 Fe and 1.0 Ti.

TABLE II. - THERMAL-MECHANICAL PROCESSING AND HEAT TREATMENT SCHEDULES

Alloy	Thermal-mechanical processing	Heat treatment
TD-Ni	(a)	(a)
DS-NiCr(S)	Extruded ~12:1 at ~1365 K by vendor	Heated from 1475 to 1617 K in 2 hr
DS-NiCr(F)	Extruded ~12:1 at ~1365 K by vendor	2 hr at 1640 K
Inconel MA-754	(a)	(a)
TD-NiCrAl	Extruded 12:1 at 1365 K to 3- by 10-cm sheet bar, hot rolled to 1.5-cm thickness in two 30-percent passes at 1365 K	2 hr at 1640 K
DST-NiCrAl	Canned in steel, extruded 16:1 at 1395 K to ~1.7-cm-diam bar	2 hr at 1640 K

[a]Not reported by vendor.

TABLE III. - GRAIN SIZE PARAMETERS AND TEXTURE OF ODS ALLOYS

(a) Grain size

Alloy	Characteristic length, μm			Average grain size, $0.85\sqrt[3]{L_1L_2L_3}$, μm	Grain aspect ratio, $L_1/\sqrt{L_2L_3}$
	Parallel to extrusion axis, L_1	Long transverse, L_2	Short transverse, L_3		
TD-Ni	25	Diam, 1.3	---	3.5	19
DS-NiCr(S)	(a)	----------	---	-----	----------
DS-NiCr(F)	(b)	----------	---	-----	----------
Inconel MA-754	530	180	115	250	3.7, [c]0.73
DST-NiCrAl	1200	Duplex diam, 600 and 120	---	400	[d]1.8
TD-NiCrAl	490	285	150	235	2.4

(b) Texture

Alloy	Orientation
TD-Ni	Wire, [100] parallel to extrusion axis
DS-NiCr(S)	[100] parallel to extrusion axis, [011] parallel to long transverse direction, [0$\bar{1}$1] parallel to short transverse direction
DS-NiCr(F)	Same as DS-NiCr(S)
Inconel MA-754	Same as DS-NiCr(S)
TD-NiCrAl	Same as DS-NiCr(S)
DST-NiCrAl	Wire, [522] parallel to extrusion axis

[a]Single crystal; large, elongated subgrains.

[b]Single crystal; large, elongated subgrains (smaller than DS-NiCr(S)) and large, elongated grains in twin orientation.

[c]Calculated for transverse testing, $\sqrt{L_2L_3}/L_1$.

[d]Calculated for larger grain diameter.

TABLE IV. - CREEP HISTORY AND ROOM TEMPERATURE RESIDUAL TENSILE PROPERTIES FOR SEVERAL ODS ALLOYS

Specimen	Creep conditions at 1365 K			Room temperature residual tensile properties				Macroscopic fracture appearance (a)
	Stress, MPa	Time, hr	Strain, percent	0.2 Percent yield strength, MPa	Ultimate tensile strength, MPa	Elongation, percent	Reduction in area, percent	
TD-Ni; tested parallel to extrusion axis								
N-50	65.5	142.4	0.49	310	395	19	84	Cup and cone, intragranular
N-53	62	120.5	.35	444	519	21	80	
N-52	58.6	141.0	.30	360	447	20	82	
N-56	55.1	148.4	.20	411	495	21.5	78	
[b]N-5	55.1	116.9	.18	404	530	24	80	
N-10	48.2	117.3	.25	338	460	18	82	
[b]N-4	48.2	120.5	.12	320	448	23	81	
Average	(c)	-----	----	441	489	19	80	
[b]N-3	(c)	-----	----	515	588	18	76	
Inconel MA-754; tested parallel to extrusion axis								
L-16	89.6	73.1	1.0	594	611	4	4.5	Intergranular, some oxide
L-13	86.1	82.5	.5	642	978	15	16.5	Shear, possibly some intergranular
L-12	82.7	69.0	~.3	628	978	15.5	15.5	Intergranular, shear
L-5	82.7	100.4	.44	637	880	8.3	12.6	Mainly intergranular, spots of oxide
L-6	79.2	146.2	.14	---	995	18.4	17.6	Intergranular, shear
L-7	75.9	141.1	.31	643	976	11	11	Shear, possibly some intergranular
L-15	75.9	47.8	.2	657	1016	16	22.5	Intragranular, shear
L-14	72.3	141.9	.11	651	973	18.5	20	
L-8	68.9	141.6	.1	632	991	22.5	21	
L-3	65.5	145.1	.12	593	996	18.7	22.5	
Average	(c)	-----	----	667	1037	21	22	
Inconel MA-754; tested parallel to long transverse direction								
T-7	34.5	67.3	1.67	(d)	164	2	----	Intergranular, almost completely oxidized, 90°
T-6	27.6	72.7	1.24	(d)	153	2	----	Intergranular, almost completely oxidized, 90°
T-1	24.1	101.0	.91	(d)	466	1.3	0.5	90°, some oxide, intergranular
T-13	22.4	94.1	~.22	624	885	12	18	90°, some shear, intergranular
T-3	20.7	120.3	.49	600	681	1.5	1.5	90°, intergranular
T-11	20.7	149.2	.06	621	832	8	12.5	90°, intergranular
T-2	18.9	148.7	.44	597	681	3	2.4	90°, intergranular
T-14	17.2	149.5	.12	593	884	12	16	90°, intergranular
T-5	13.8	148.3	0	664	896	15.5	16	90°, intergranular
Average	(c)	-----	----	656	934.7	23	27.5	Intragranular, shear

DS-NiCr(S); tested parallel to extrusion axis								
S-3	79.2	98.3	1.64	410	769	26	36	Elliptical cross section, shear
S-5	75.9	115.1	.60	411	788	26	41	
S-9	72.3	101.4	.30	414	789	26	27.5	
S-8	68.9	500	.2	396	792	23.5	36	
S-12	68.9	115.7	.08	434	786	26	34	
S-13	65.5	101.0	.18	401	759	25	40.5	
S-14	62	119.5	.13	399	782	27	40	
Average	(c)	-----	----	390	796	24	31.5	
DS-NiCr(S); tested parallel to long transverse direction								
ST-11	82.7	88.6	0.32	423	591	15	15	Shear, some 90°
ST-9	68.9	146.2	.1	408	606	33	46	Shear, elliptical cross section
ST-7	62.0	150.3	.15	430	630	40.5	46	
ST-4	27.6	147.9	.03					
ST-4[e]	55.1	146.7	.07	404	601	30	49	
ST-5	24.1	141.1	0					
ST-5[e]	48.2	135.3	.02	391	615	32	42	
ST-3	34.5	148.6	0	424	620	26	42.5	
ST-2	31.0	150.3	0	411	616	37.5	44.5	
ST-10	(c)	-----	----	442	626	42	43	
DS-NiCr(F); tested parallel to extrusion axis								
F-6	72.4	150	0.19	416	711	11.8	18.5	Shear, possible small intergranular, elliptical
F-5	62.0	148.3	.1	408	795	22	25	Shear, elliptical
F-2	62.0	149.3	.44	---	263	2	----	Out of gage, intergranular, oxidized
F-4	(c)	-----	----	406	790	26	38	Shear, elliptical cross section
TD-NiCrAl; tested parallel to extrusion axis								
TL-9	55.1	74.8	1.8	(d)	268	2	--	Intergranular, almost completely oxidized
TL-7	55.1	44.0	.57	769	800	3	4	Partial intergranular, some oxide
TL-12	51.7	115.7	.11	775	1108	8	15	Intragranular, 90°, shear lip
TL-3	(c)	-----	----	785	1181	11	10	Intragranular, 90°, shear lip
DST-NiCrAl; tested parallel to extrusion axis								
T-8-8	62.0	102	3.46	605	605	2.7	----	Intergranular, oxidized
T-8-6	55.1	142.2	.68	750	755.8	1.8	----	Mainly intergranular, cracks some oxide
T-8-7	48.2	140.3	.28	706	834.4	5.4	10	Partially intergranular, cracks
T-8-12	44.8	168	.3	674.5	1033	13	12	Small area of intergranular, cracks
T-8-4	41.3	148.9	.24	737	1030	11	11.5	Shear, cup and cone, intergranular
T-8-3	41.3	150.1	.18	698	999	13	15	Very small region of intergranular, small area of oxide
Average	(c)	-----	----	748	1088	15	15	Cup and cone, intragranular

[a]Shear denotes fracture surface ~45° to stress axis; 90° denotes fracture surface perpendicular to stress axis.

[b]Plasma coated with Ni-20Cr, ~100 μm thick.

[c]As-received.

[d]Did not yield

[e]Load increased.

TABLE V. - CREEP HISTORY AND 1365 K RESIDUAL TENSILE PROPERTIES FOR SEVERAL ODS ALLOYS

[Alloys tested parallel to extrusion axis.]

Specimen	Creep conditions			1365 K residual tensile properties				Macroscopic fracture appearance
	Stress, MPa	Time, hr	Strain, percent	0.2 Percent yield strength, MPa	Ultimate tensile strength, MPa	Elongation, percent	Reduction in area, percent	
TD-NiCrAl								
TL-10	48.2	118.	0.12	94.4	100.6	7.5	15	Partially intergranular, round cross section
TL-6	44.8	115.8	.05	88.2	95.8	7.3	16.5	Partially intergranular, elliptical cross section
TL-8	41.3	114.2	.10	98.5	105.4	18	37	Partially intergranular, elliptical cross section
Average	(a)	-----	----	100.3	106.5	20	44.5	Intragranular, elliptical cross section
DST-NiCrAl								
T-9-3	55.1	137.9	0.51	86	91	5.5	8.5	Intergranular
T-9-2	51.7	163.9	.3	83	93	6.5	8.5	
T-9-4	48.2	118.9	.19	85	91	3.5	7.5	
T-9-7	44.8	165.8	.25	84	92	7.5	7	
T-9-6	42.3	146.8	.27	85	94	10.5	17	
T-9-5	41.3	147.8	0	86	94	3.5	4	
Average	(a)	-----	----	85	96	11	13	

[a]As-received.

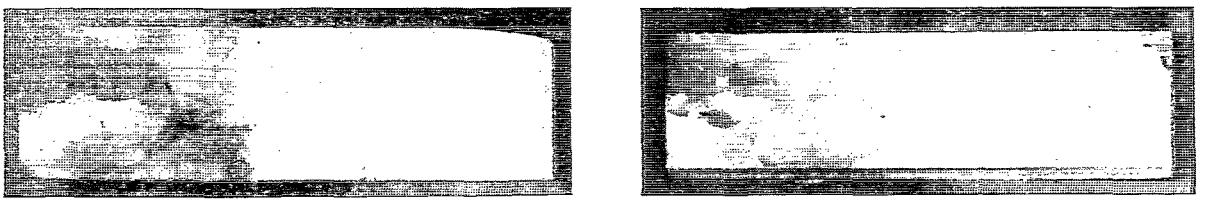

CS-77362

5.1 cm

(a) DS-NiCr(S); heat treatment: 1477 to 1617 K in 2 hours.

(b) DS-NiCr(F); heat treatment: 1640 K for 2 hours.

Figure 1. - Photomacrographs of cross sections of extruded and heat-treated DS-NiCr bar. Macroetchant: 70 percent HCl, 30 percent H_2O_2.

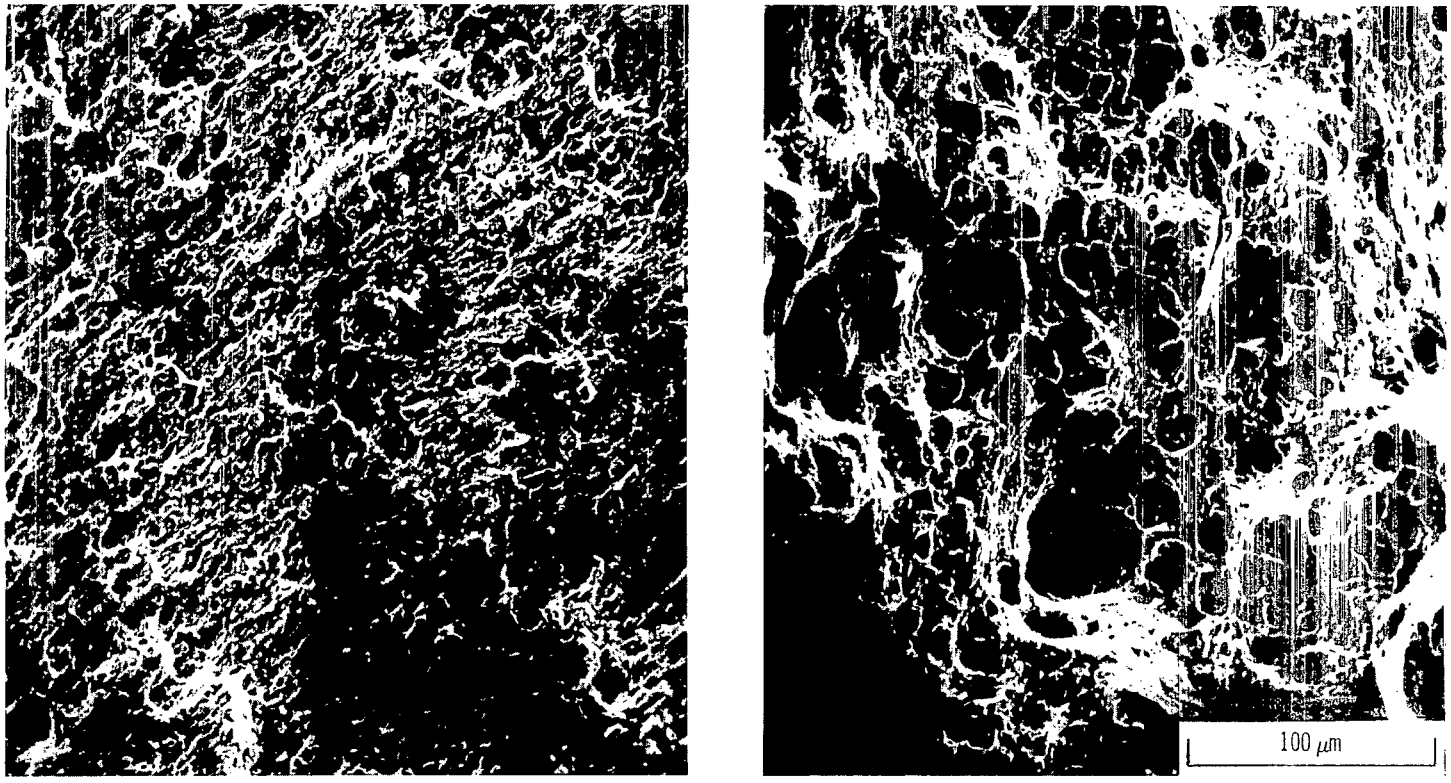

CS-73364

(a) As-received.

(b) Creep tested at 1365 K and 82.7 MPa for 100.4 hours with 0.44 percent strain.

Figure 2. - Typical SEM fractographs of room temperature tensile fracture surfaces of Inconel MA-754 tested parallel to extrusion axis.

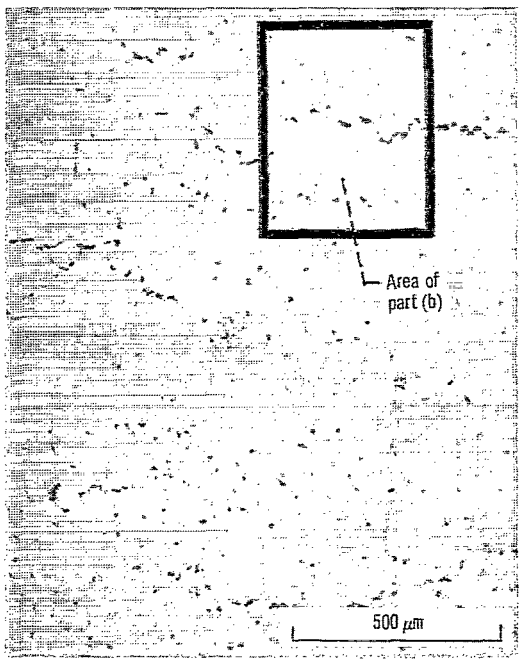

(a) Gross intergranular creep damage

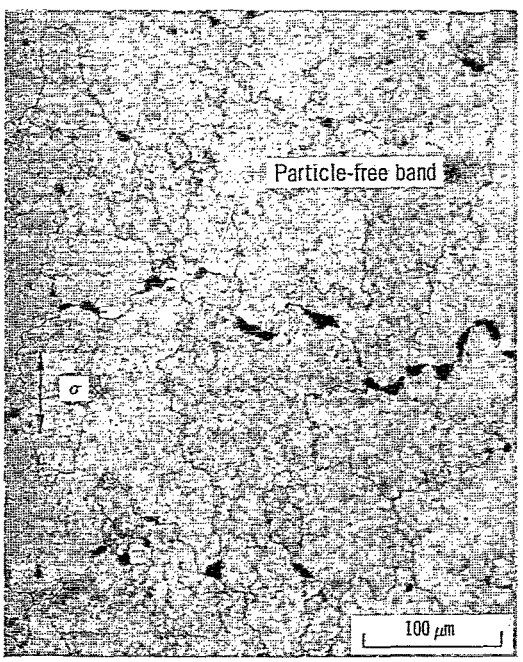

(b) Dispersoid (Y_2O_3) - free band developed by diffusional creep mechanisms.

Figure 3. - Photomicrographs of Inconel MA-754 tested in long transverse direction. Specimen tensile tested at room temperature following creep testing at 1365 K and 24.1 MPa for 101.0 hours with 0.91 percent strain. Electrolytically stain etched with chromic acid mixture (100 cm^3 H_2O, 100 cm^3 H_2SO_4, 2 g chromic acid).

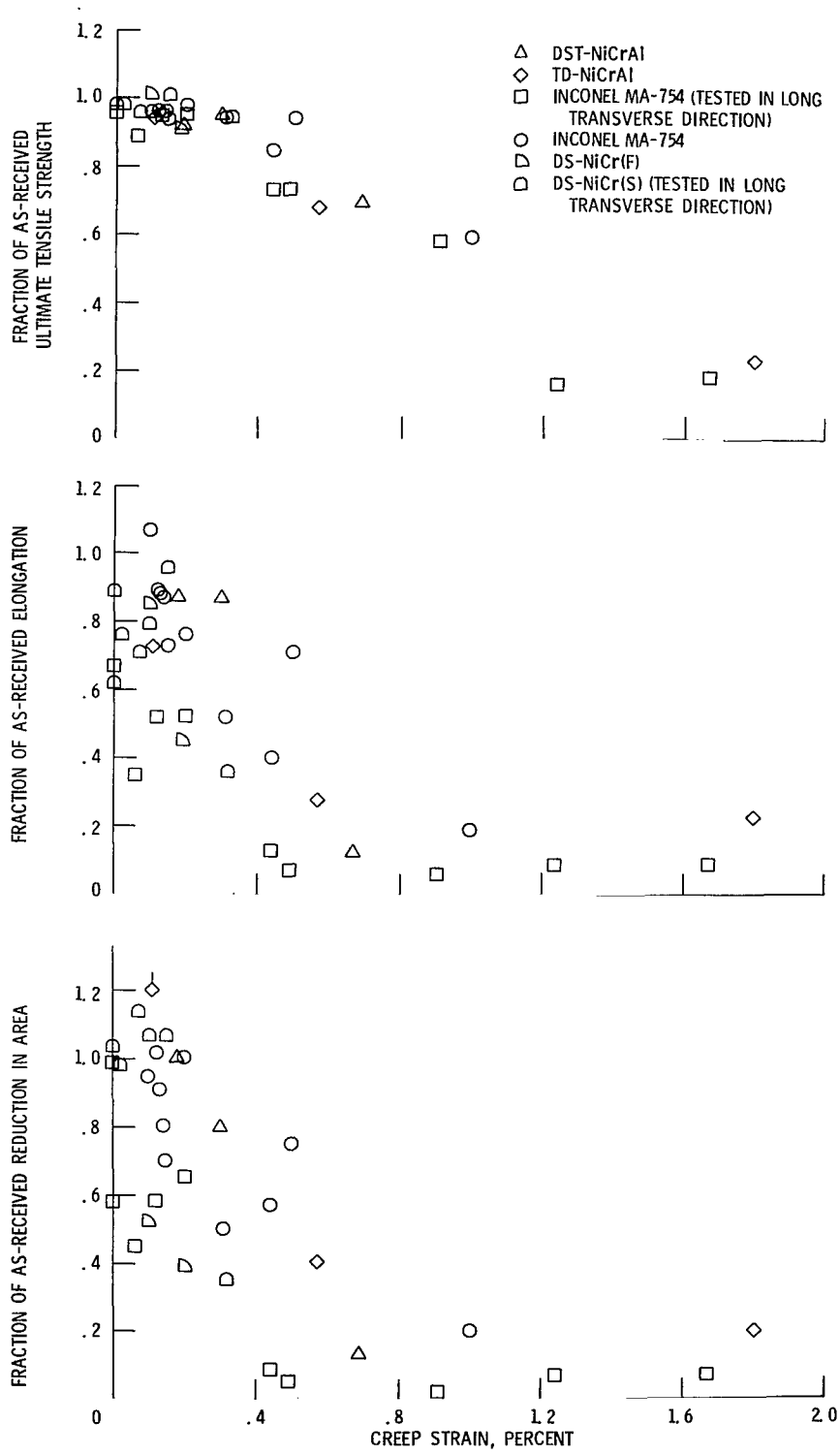

Figure 4. - Normalized room temperature tensile properties as function of prior creep strain at 1365 K.

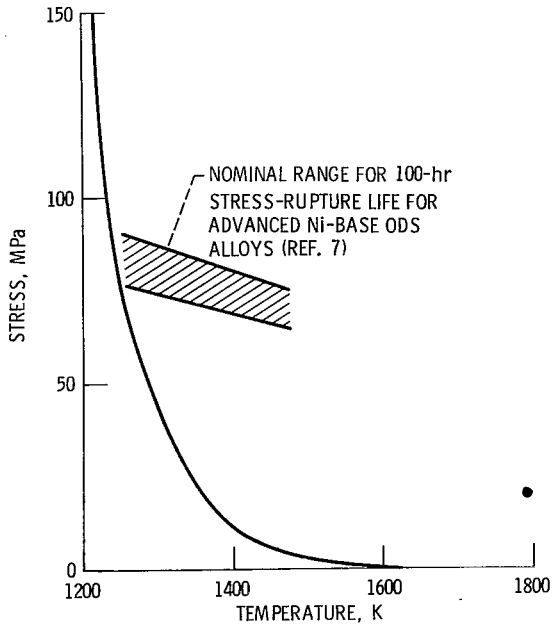

Figure 5. - Theoretical stress and temperature conditions to produce 1 percent creep in 100 hours by diffusional creep in 250-micrometer-grain-size ODS-Ni alloy and 100-hour stress-rupture life for advanced Ni-base ODS alloys.

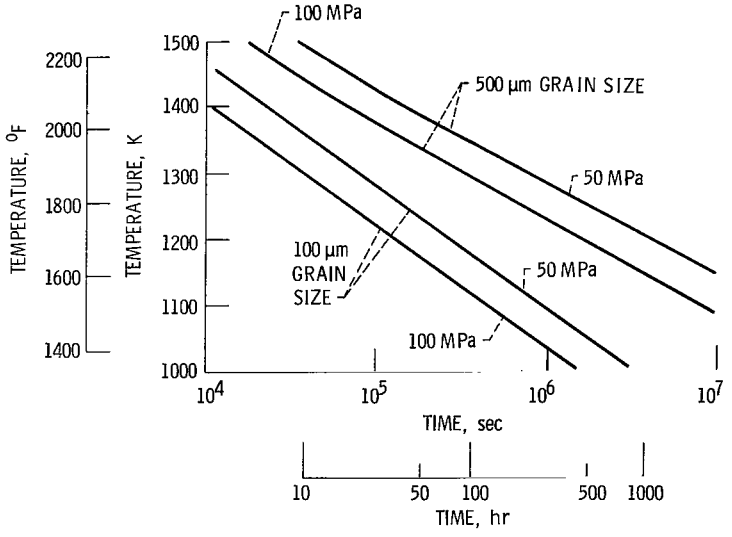

Figure 6. - Stress, temperature, and time conditions necessary to produce 2-micrometer-thick dispersoid-free band by diffusional creep in ODS-Ni alloys.

(a) As-received.

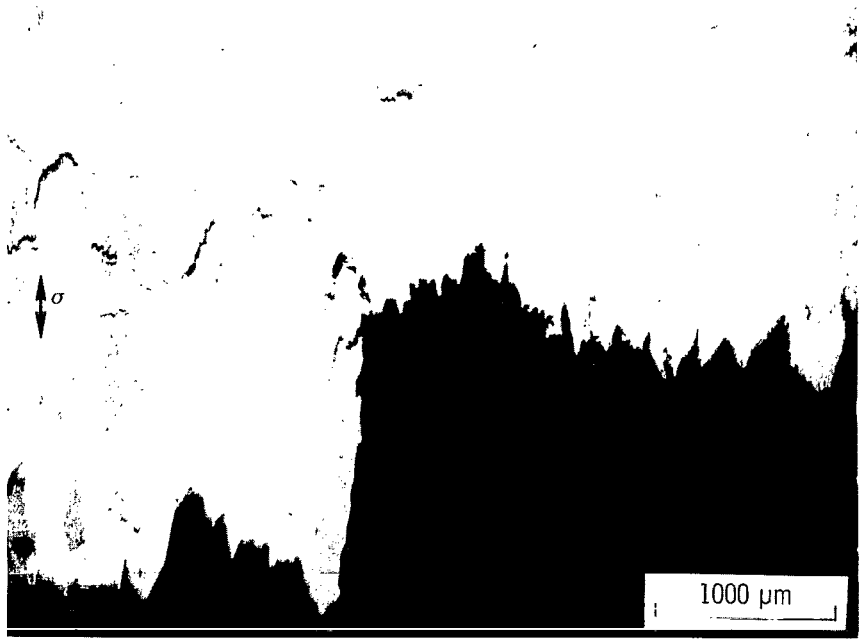

(b) Creep tested at 1365 K and 48.2 MPa for 118 hours with 0.12 percent strain.

Figure 7. - Photomicrographs of 1365 K tensile fracture of TD-NiCrAl tested parallel to extrusion axis.

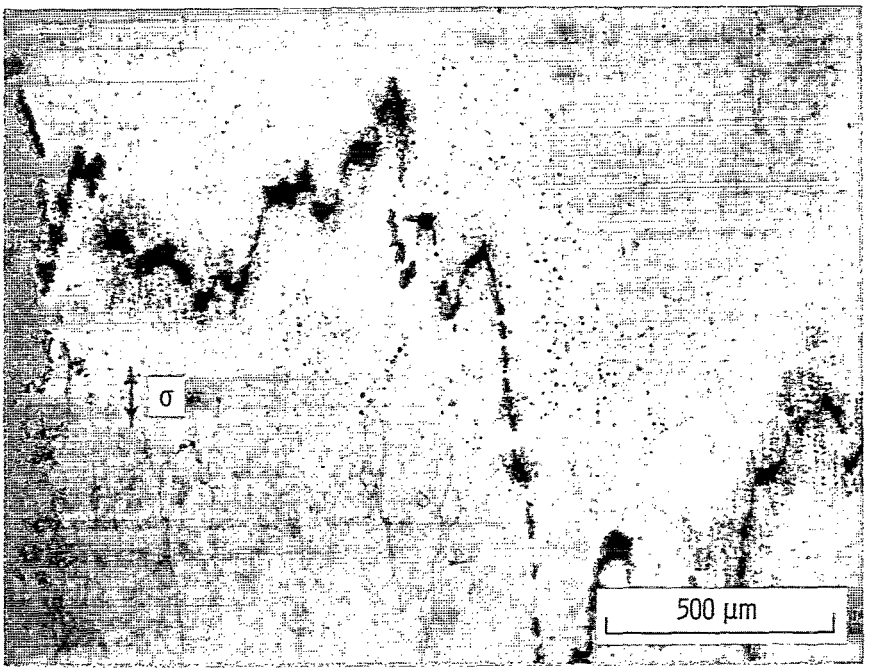

Figure 8. - Creep damage in DST-NiCrAl tested parallel to extrusion axis. Specimen creep tested at 1365 K and 55.1 MPa for 137.9 hours with 0.51 percent strain, then tensile tested at 1365 K.

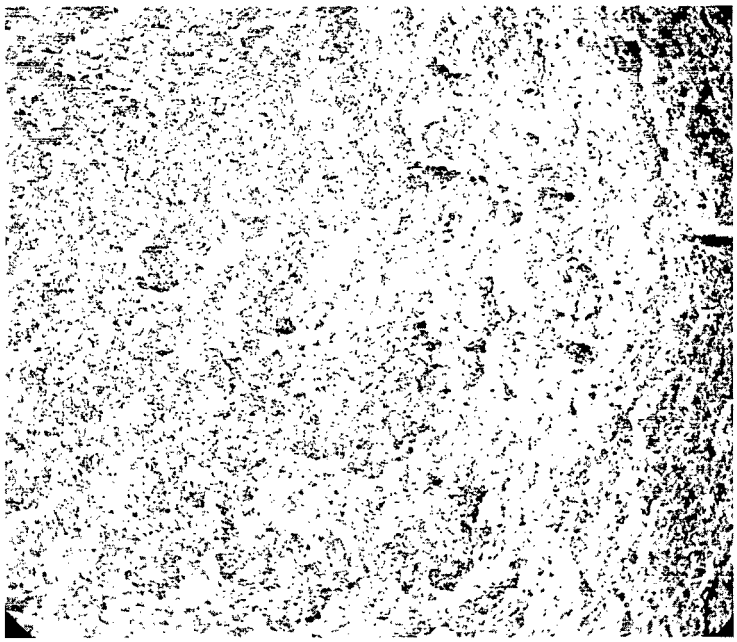

(a) As-received.

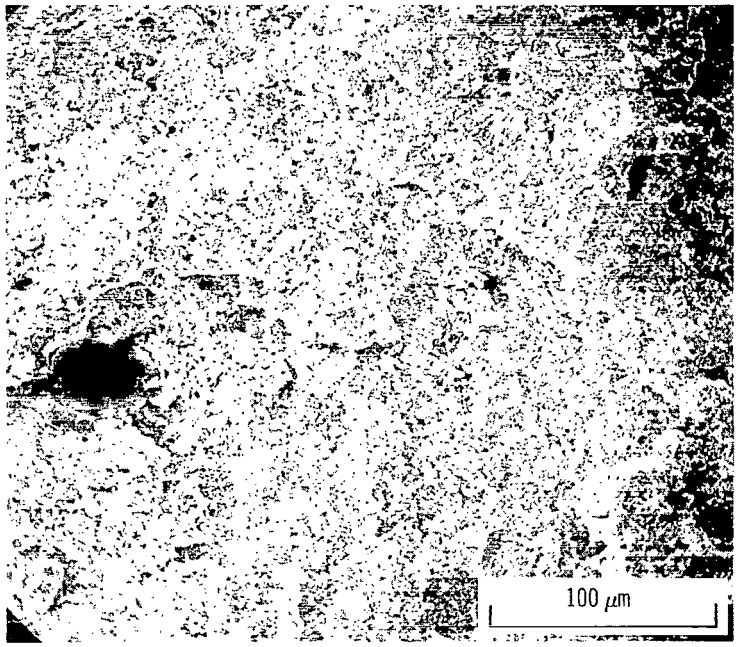

(b) Creep-tested at 1365 K and 62 MPa for 142.4 hours with 0.49 percent strain.

Figure 9. - Typical SEM fractographs of room temperature tensile specimens of TD-Ni tested parallel to extrusion axis.

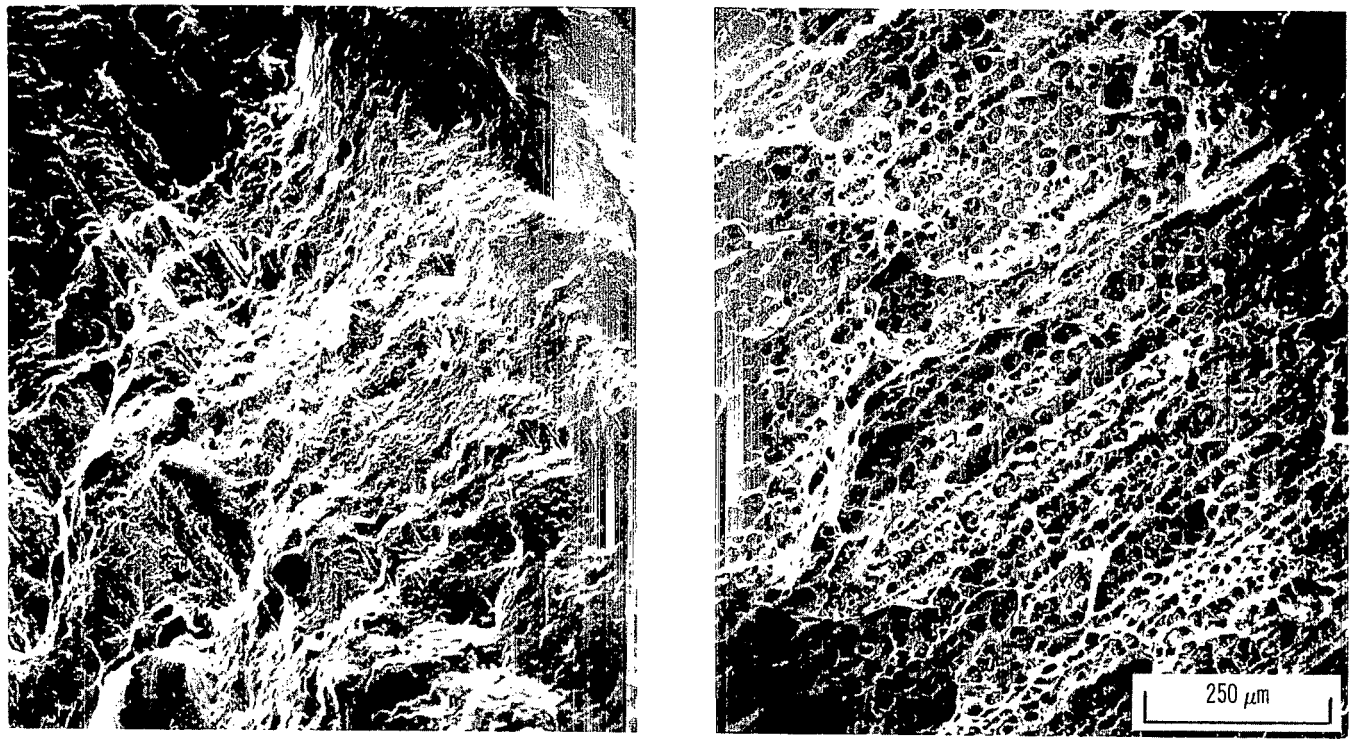

(a) As-received.

(b) Creep-tested at 1365 K and 18.9 MPa for 148.7 hours with 0.44 percent strain.

Figure 10. - Typical SEM fractographs of room temperature tensile specimens of Inconel MA-754 tested in long transverse direction.

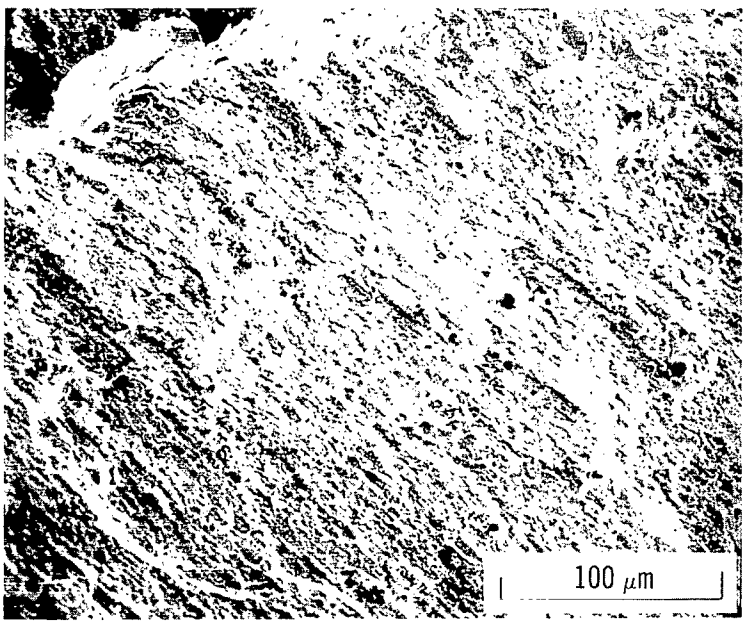

Figure 11. - Typical SEM fractograph of room temperature tensile fracture surface of DS-NiCr(S) tested parallel to extrusion axis.

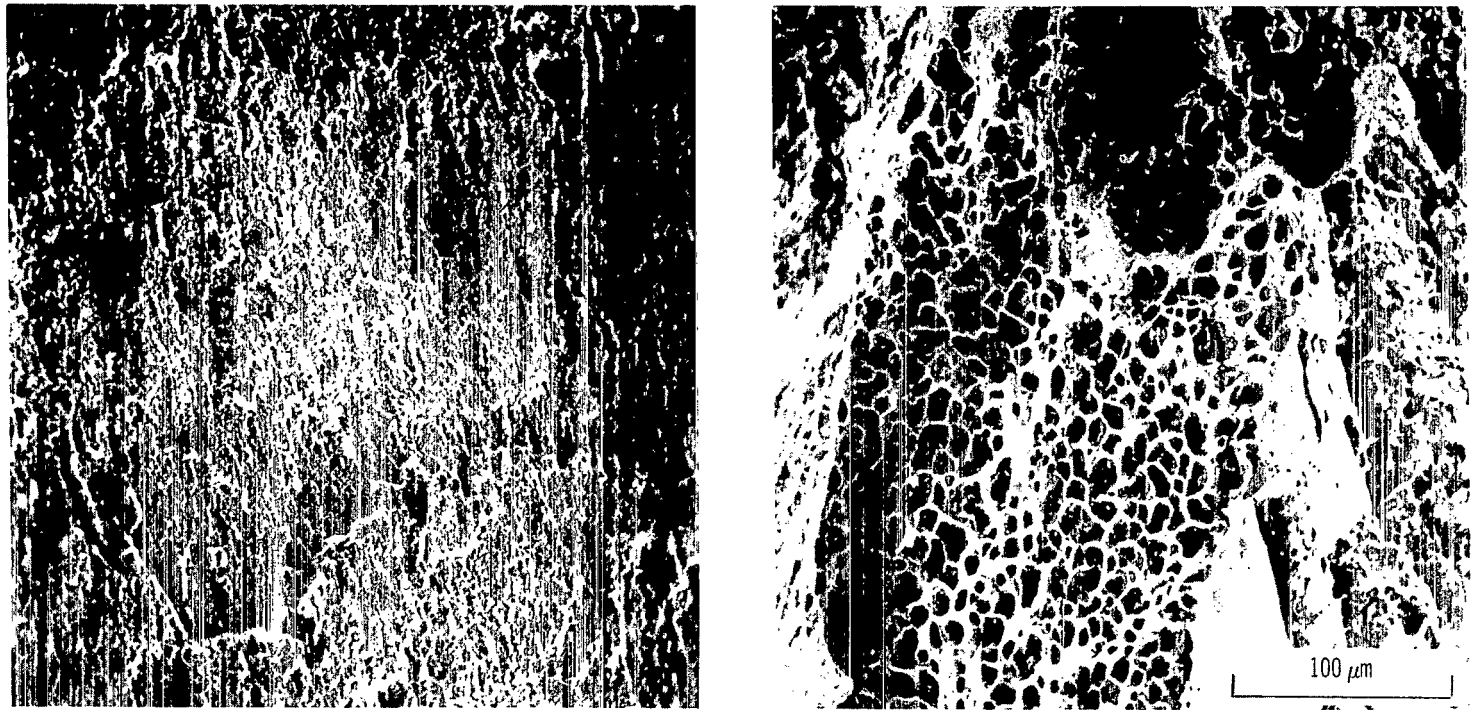

CS-77363

(a) As-received.

(b) Creep-tested at 1365 K and 82.7 MPa for 88.6 hours with 0.32 percent strain.

Figure 12. - Typical SEM fractograph of room temperature tensile specimens of DS-NiCr(S) tested in long transverse direction.

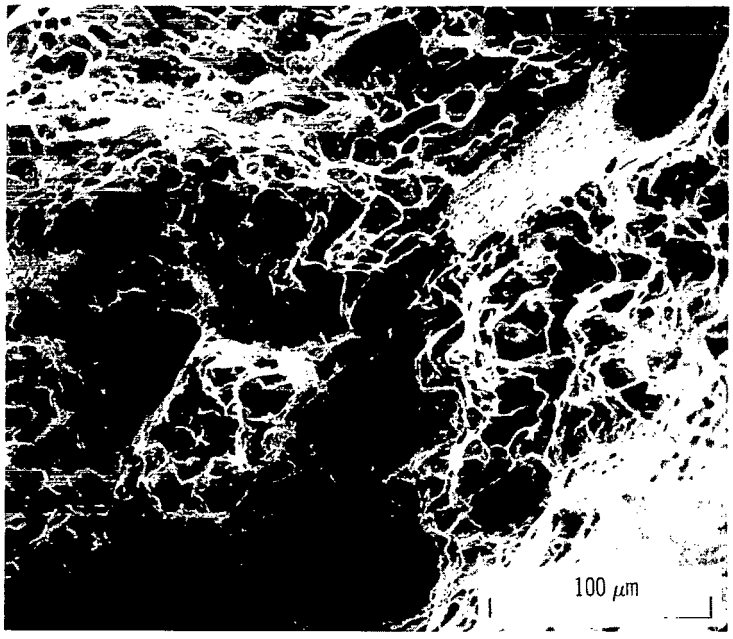

Figure 13. - SEM fractograph of room temperature tensile fracture surface of DS-NiCr(F) which had been previously creep tested at 1365 K and 72.4 MPa for 150 hours with 0.19 percent strain.

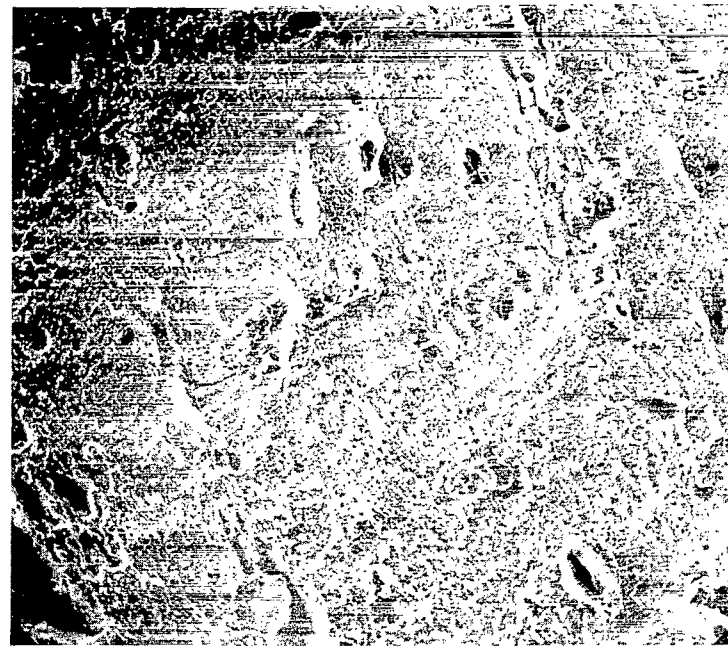

(a) Creep-tested at 1365 K and 51.7 MPa for 115.7 hours with 0.11 percent strain.

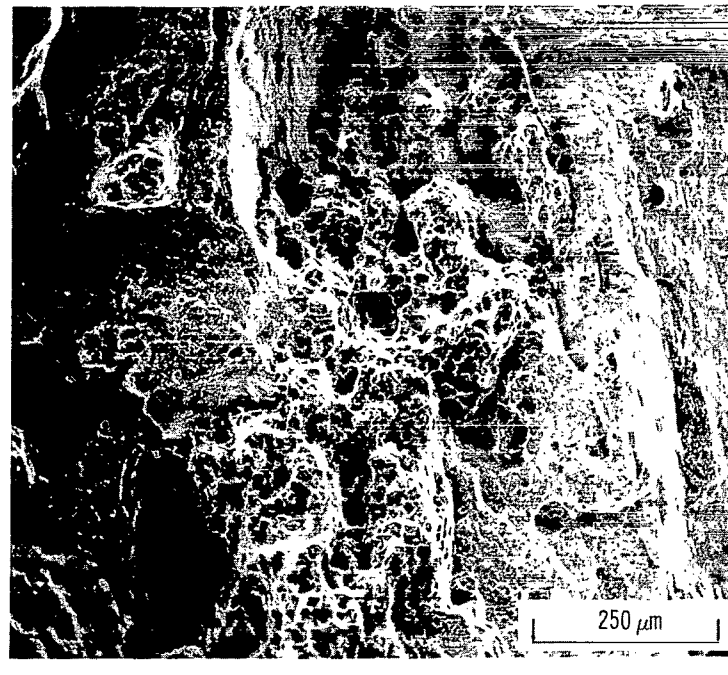

(b) Creep-tested at 1365 K and 55.1 MPa for 44.0 hours with 0.57 percent strain.

Figure 14. - Typical SEM fractographs of room temperature tensile specimens of TD-NiCrAl creep-tested parallel to extrusion axis.

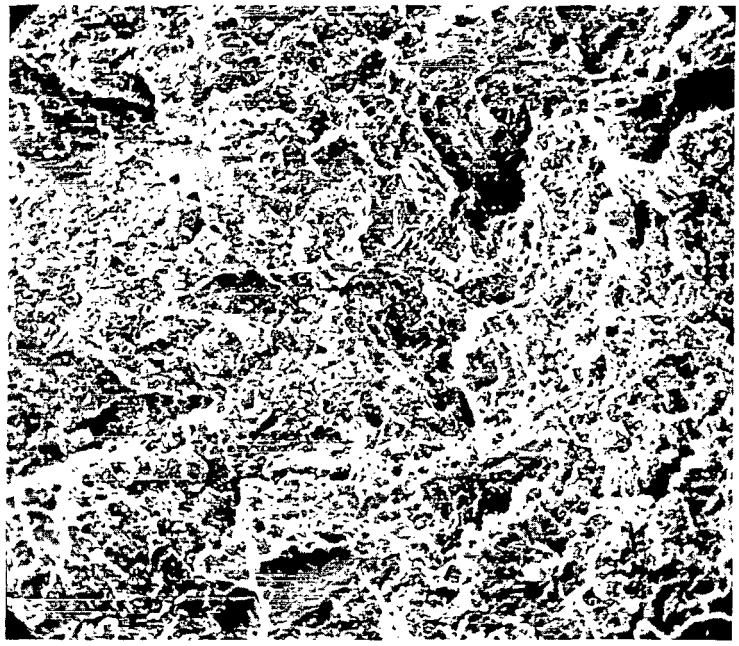

(a) As-received.

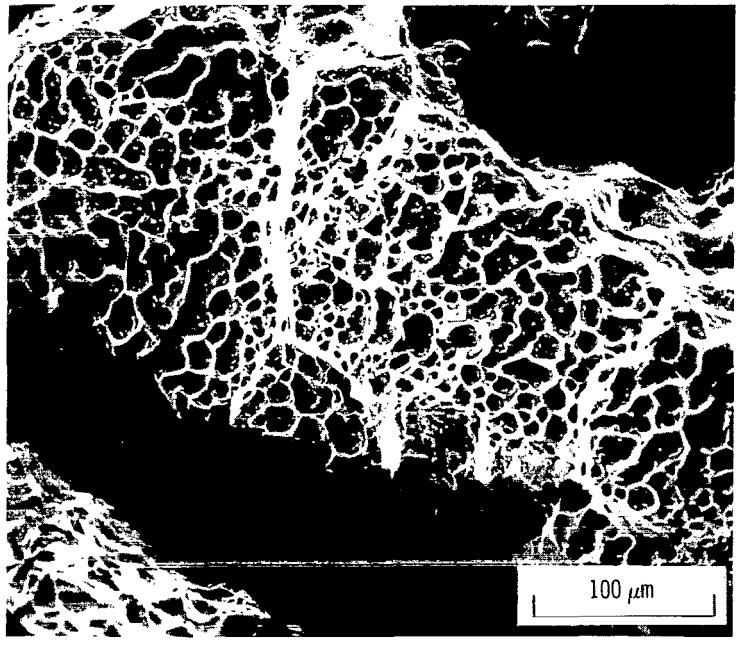

(b) Creep-tested at 1365 K and 48.2 MPa for 140.3 hours with 0.28 percent strain.

Figure 15. - Typical SEM fractographs of room temperature tensile specimens of DST-NiCrAl tested parallel to extrusion axis.

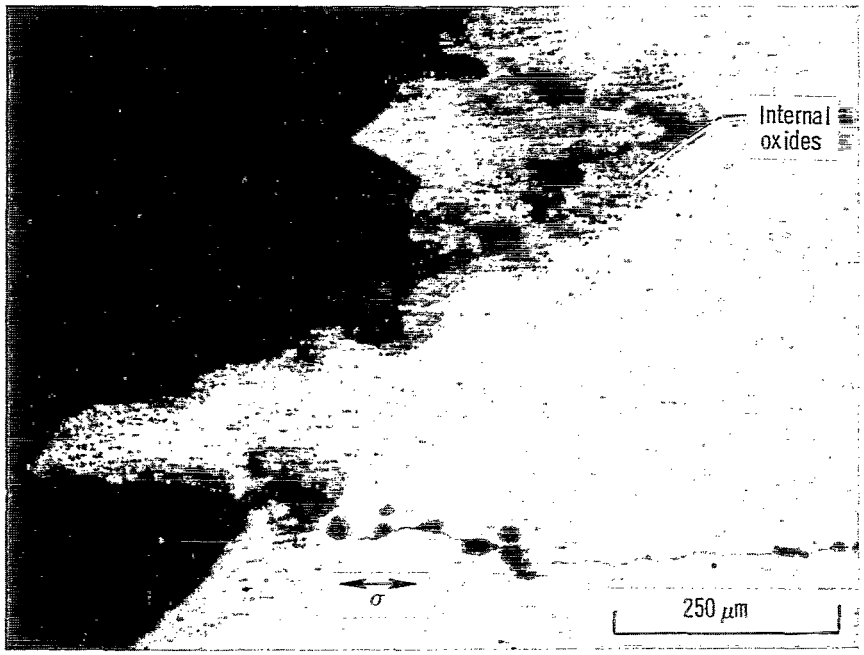

Figure 16. - Photomicrograph of portion of room temperature residual tensile fracture surface of DST-NiCrAl specimen which had been previously creep-tested at 1365 K and 55.1 MPa for 142.2 hours with 0.68 percent strain.

NATIONAL AERONAUTICS AND SPACE ADMINISTRATION
WASHINGTON, D.C. 20546

OFFICIAL BUSINESS
PENALTY FOR PRIVATE USE $300

SPECIAL FOURTH-CLASS RATE BOOK

POSTAGE AND FEES PAID
NATIONAL AERONAUTICS AND SPACE ADMINISTRATION
451

U.S.MAIL

"The aeronautical and space activities of the United States shall be conducted so as to contribute . . . to the expansion of human knowledge of phenomena in the atmosphere and space. The Administration shall provide for the widest practicable and appropriate dissemination of information concerning its activities and the results thereof."

—NATIONAL AERONAUTICS AND SPACE ACT OF 1958

NASA SCIENTIFIC AND TECHNICAL PUBLICATIONS

TECHNICAL REPORTS: Scientific and technical information considered important, complete, and a lasting contribution to existing knowledge.

TECHNICAL NOTES: Information less broad in scope but nevertheless of importance as a contribution to existing knowledge.

TECHNICAL MEMORANDUMS: Information receiving limited distribution because of preliminary data, security classification, or other reasons. Also includes conference proceedings with either limited or unlimited distribution.

CONTRACTOR REPORTS: Scientific and technical information generated under a NASA contract or grant and considered an important contribution to existing knowledge.

TECHNICAL TRANSLATIONS: Information published in a foreign language considered to merit NASA distribution in English.

SPECIAL PUBLICATIONS: Information derived from or of value to NASA activities. Publications include final reports of major projects, monographs, data compilations, handbooks, sourcebooks, and special bibliographies.

TECHNOLOGY UTILIZATION PUBLICATIONS: Information on technology used by NASA that may be of particular interest in commercial and other non-aerospace applications. Publications include Tech Briefs, Technology Utilization Reports and Technology Surveys.

Details on the availability of these publications may be obtained from:

SCIENTIFIC AND TECHNICAL INFORMATION OFFICE

NATIONAL AERONAUTICS AND SPACE ADMINISTRATION

Washington, D.C. 20546